CHEMICAL ENGINEERING TRANSACTIONS
VOL. 74, 2019
A publication of AIDIC
The Italian Association of Chemical Engineering
Online at www.cetjournal.it
Guest Editors: Sauro Pierucci, Jiří Jaromír Klemeš, Laura Piazza

ISBN 978-88-95608-71-6; **ISSN** 2283-9216
DOI: 10.3303/CET1974187

Process Parameters Optimal Investigation on the Na_2SO_4 Fractional Crystallization from Coal Chemical Industry High-Saline Wastewater

Chao Bian, Hang Chen, Xingfu Song*, Jianguo Yu

State Environmental Protection Key Laboratory of Environmental Risk Assessment and Control on Chemical Process, East China University of Science and Technology, Shanghai 200237, China
xfsong@ecust.edu.cn

The fractional crystallization process of high-saline wastewater is important for the sustainable development of coal chemical industry. This study mainly focused on the process investigation of Na_2SO_4 crystallization separation. The effects of heating temperature and stirring rate on the particle size distribution of anhydrous sodium sulphate (Na_2SO_4) crystals were investigated by batch-evaporation crystallization. Taking into account the product performance and the operating costs, the optimal operating conditions were determined to be 130 °C and 300 rpm. Granular Na_2SO_4 crystals with a purity higher than 99.0% were obtained. And the corresponding $D_{0.10}$ was 309 μm. Moreover, the effects of impurity ions and organic matter on the preparation of Na_2SO_4 were discussed. The experimental results reveal that the addition of impurity, whether ions or organic matter, can lead to a decrease of $D_{0.10}$. Specially, $D_{0.10}$ increases with the increasing wt.%(K^+), while $D_{0.10}$ gradually decreases as wt.%(F^-) increases. Furthermore, the influence level of organic matter on $D_{0.10}$ was ranked as tributyl phosphate> 4-methyl-2-pentanone> dodecane> p-nitrophenol. The corresponding SEM images show that the addition of 10 mM of these four substances have little effect on the crystal morphology.

1. Introduction

China is rich in coal, poor in oil and lean in gas, which determines the rapid development of coal chemical industry and leads to the massive discharge of high-saline wastewater. Meanwhile, the distributions of coal resource and water resource are extremely uneven. Western China is not only a place rich in coal resources, but also a scarce place for water resources. Therefore, poor water resource situation and severe water environment problems have become the bottleneck, which restricts the development of local coal chemical industry. Generally, high-saline wastewater contains large amounts of inorganic salt ions, colloids, suspended matter and even refractory organic pollutants. With the implementation of the stringent water resource management, “zero discharge” of wastewater from coal chemical enterprises has been proposed. More and more attentions have been paid to the recycling of inorganic salts, namely, the fractional crystallization process.

On the basis of water quality analysis, the typical inorganic system of high-saline wastewater from coal chemical industry is NaCl-$NaNO_3$-Na_2SO_4-H_2O. Up to now, there have been a series of researches on the phase equilibria of this quaternary system. The stable phase equilibrium data of NaCl-$NaNO_3$-Na_2SO_4-H_2O system at low temperatures (258.15, 268.15, 273.15 and 278.15 K) were measured by isothermal dissolution equilibrium method (Zhang and Huang, 2015). The phase diagrams of the quaternary system at 353.15 (Bian et al., 2018) and 373.15 K (Yang et al., 2017) were plotted. In addition, the metastable phase equilibrium of the same system at 298.15 and 323.15 K were measured by the isothermal evaporation method (Lin et al., 2011). Meanwhile, the thermodynamic models have been widely used to calculate the equilibrium of related salt water systems. For example, part of the Pitzer parameters for the system Na^+//Cl^-, NO_3^-, SO_4^{2-}-H_2O at 298.15 K were regressed by fitting the experimental data (Song and Huang, 2007). These thermodynamic studies provide essential data for the flowsheet design of the fractional crystallization. However, related crystallization process investigation is few.

Paper Received: 6 March 2018; Revised: 13 August 2018; Accepted: 3 January 2019

Please cite this article as: Bian C., Chen H., Song X., Yu J., 2019, Process Parameters Optimal Investigation on the Na2so4 Fractional Crystallization from Coal Chemical Industry High-saline Wastewater, Chemical Engineering Transactions, 74, 1117-1122
DOI:10.3303/CET1974187

According to the fundamental phase equilibrium data, we have proposed a reasonable separating route previously, in which Na_2SO_4, NaCl and $NaNO_3$ can be recycled by evaporation-cooling crystallization processes. This paper mainly focuses on the process investigation of Na_2SO_4 fractional crystallization. It is aimed at investigating the effects of heating temperature, stirring rate, impurity ions and organic matter on the evaporation crystallization process of Na_2SO_4, providing an experimental basis for the optimal operating conditions.

2. Materials and methods

2.1 Materials

Sodium sulfate (analytical reagent grade, AR, ≥99.0%), sodium chloride (AR, ≥99.5%) and sodium nitrate (AR, ≥99.0%) purchased from Sinopharm Chemical Reagent Co. Ltd. (Shanghai, China) were used to prepare the simulation liquid of high-saline wastewater without further treatment. Tributyl phosphate, 4-methyl-2-pentanone, dodecane and p-nitrophenol (Titan Scientific Co., Ltd., Shanghai, China) were added as the typical organic pollutants. The deionized water with conductivity less than 1 μS/cm was employed in all experiments.

2.2 Analytical and observation methods

The structure and composition of the products were identified by powder X-ray diffractometer (XRD; D8 advanced, Bruker, Germany) using Cu Kα radiation with a scanning rate of $10°\cdot min^{-1}$ and a scanning 2θ range of 10 to 80°. The laser particle size analyser (Mastersizer 3000, Malvern, UK) was employed to analyse the particle size distribution of the products. And the scanning electron microscopy (SEM; Quanta 250, FEI Co., US) was applied to characterize the morphology of the crystals.

2.3 Experimental methods

The experimental apparatus for evaporation crystallization process was shown in Figure 1. All experiments were carried out in a jacketed glass vessel with a volume of 500 mL. The temperature (110-180 □) was controlled by a programmable temperature controlled thermostat (FP 50, Julabo, Germany) with bath oil (Thermal H10, Julabo, Germany). Besides, the quality of the evaporated water was measured by the analytical balance (± 0.01 g) in real time.

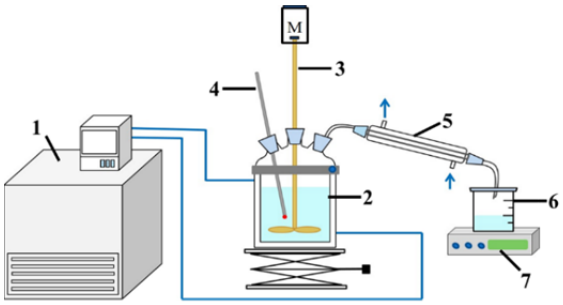

Figure 1: Experimental apparatus for batch-evaporation crystallization: 1- thermostat; 2- jacketed glass vessel; 3- stirrer; 4- mercurial thermometer; 5- condensing unit; 6- condensate receiver; 7- analytical balance

Based on the phase equilibrium data of the quaternary system $Na^+//Cl^-$, NO_3^-, SO_4^{2-}-H_2O, the starting point and end point of the crystallization process were determined to be the crystallization point of Na_2SO_4 and the co-crystallization point of Na_2SO_4 and NaCl, respectively. The specific composition of a certain high-saline wastewater and the critical control points were listed in Table 1. In order to ensure the purity of Na_2SO_4 products, the final quality of the evaporated water should be controlled at 40% of the water addition.

Table 1: The composition of raw water and critical control points of evaporation crystallization process

Sample	wt.%			
	Na_2SO_4	NaCl	$NaNO_3$	H_2O
Raw water	10.30	6.30	2.60	80.80
Crystallization point of Na_2SO_4	14.33	9.09	3.72	72.86
Co-crystallization point of Na_2SO_4 and NaCl	3.67	22.01	9.69	64.63

3. Results and discussion

A series of batch-evaporation crystallization experiments were carried out under different conditions. The effects of heating temperature, stirring rate, impurity ions and organics on the crystallization process were discussed as follows. It's worth mentioning that $D_{0.10}$ is an index worthy of attention in engineering application, because it has certain guiding significance for the design and selection of the filter unit.

3.1 Effect of heating temperature on evaporation crystallization process

The heating temperature of bath oil determines the evaporation efficiency. As shown in Figure 2, as the quality of evaporated water increases, the boiling point of the solution rises slightly, which leads to the gradual deviation of the linear relationship between evaporation and time, especially at low heating temperatures.

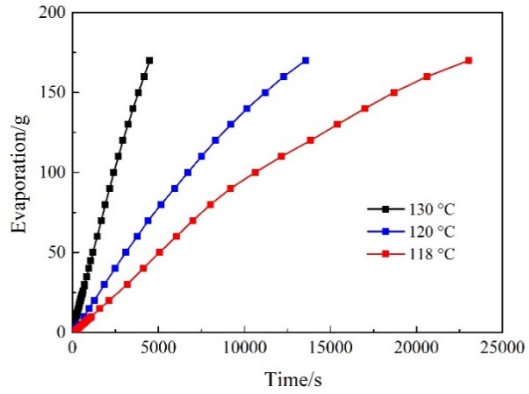

Figure 2: The relationship between evaporation and time at different temperatures

The experiments of evaporation crystallization were conducted at six different temperatures (115, 118, 120, 130, 140, 150 ˚C) with the stirring rate of 300 rpm. Afterwards, the composition and particle size distribution of the products were characterized.

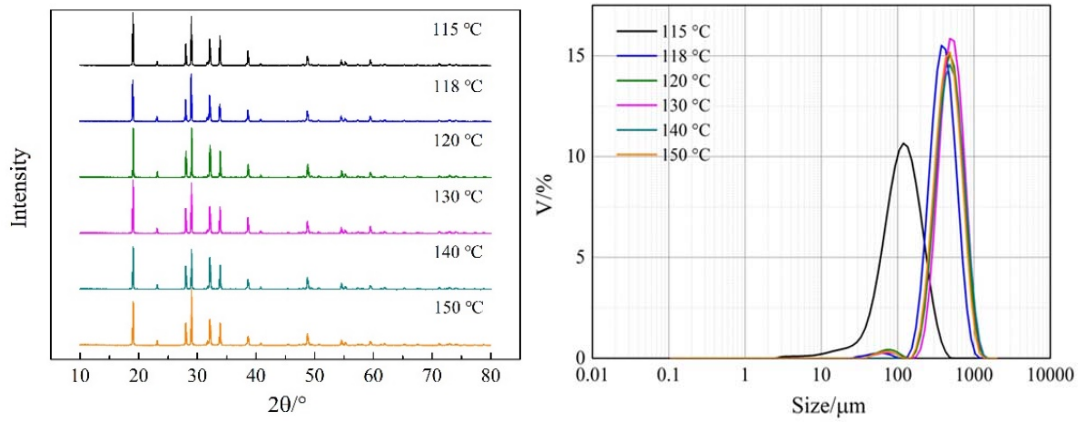

a *b*

Figure 3: XRD pattern and particle size distribution graph of Na_2SO_4 products at different temperatures with 300 rpm: a, XRD pattern; b, particle size distribution graph

Table 2: Particle size distribution of Na_2SO_4 products at different temperatures with 300 rpm

Heating temperature/ ˚C	$D_{0.10}$/μm	$D_{0.16}$ /μm	$D_{0.50}$ /μm	$D_{0.84}$ /μm	D(4,3)/μm	C.V./%
115	49.9	61.8	114	197	128	59.30
118	236	263	388	565	411	38.92
120	278	315	474	696	499	40.19
130	309	343	502	724	529	37.95
140	284	318	479	716	513	41.54
150	271	304	455	663	480	39.45

As shown in Figure 3a, all products under various conditions are Na_2SO_4 crystals. Moreover, the purities of unwashed Na_2SO_4 products were all over 99.0% by gravimetric method. Figure 3b showed the granularity distribution of the products. According to the experimental data in Table 2, $D_{0.10}$ increases with increasing temperature and reaches maximum at 130 ˚C, and then it decreases gradually. Moreover, the average particle size D(4,3) is relatively large and the coefficient of variation C.V. is relatively small at 130 ˚C. On consideration of the effect of heating temperature on evaporation efficiency and the particle size distribution of Na_2SO_4 products, 130 ˚C was determined as the optimal temperature.

3.2 Effect of stirring rate on evaporation crystallization process

The effect of stirring rate on evaporation crystallization process was investigated at 130 ˚C. As shown in Figure 4 and Table 3, $D_{0.10}$ and D(4,3) gradually increase with the increasing stirring rate from 50 to 300 rpm. There's little difference in particle size distribution at 300 and 400 rpm. When stirring rate increases to 500 rpm, $D_{0.10}$ and D(4,3) has a downward trend. It may be explained by the statement that excessive stirring exacerbates particle fragmentation. Take consideration of the energy consumption of mechanical stirring and the size distribution of Na_2SO_4 products, 300 rpm was selected as the optimal stirring rate.

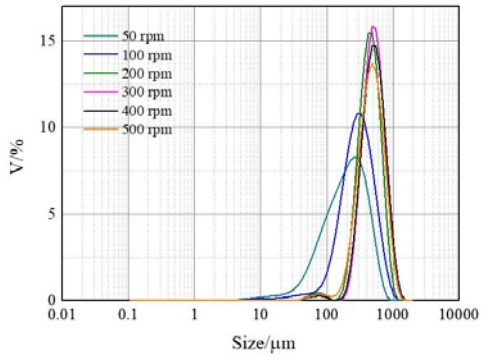

Figure 4: Particle size distribution graph of Na_2SO_4 products at 130 ˚C with different stirring rates

Table 3: Particle size distribution of Na_2SO_4 products at 130 ˚C with different stirring rates

Stirring rate/rpm	$D_{0.10}$/μm	$D_{0.16}$ /μm	$D_{0.50}$ /μm	$D_{0.84}$ /μm	D(4,3)/μm	C.V./%
50	63.9	83.5	200	384	230	75.13
100	132	162	292	496	325	57.19
200	263	296	440	637	461	38.75
300	309	343	502	724	529	37.95
400	300	337	507	749	539	40.63
500	255	294	467	710	497	44.54

3.3 Effect of impure ions on evaporation crystallization process

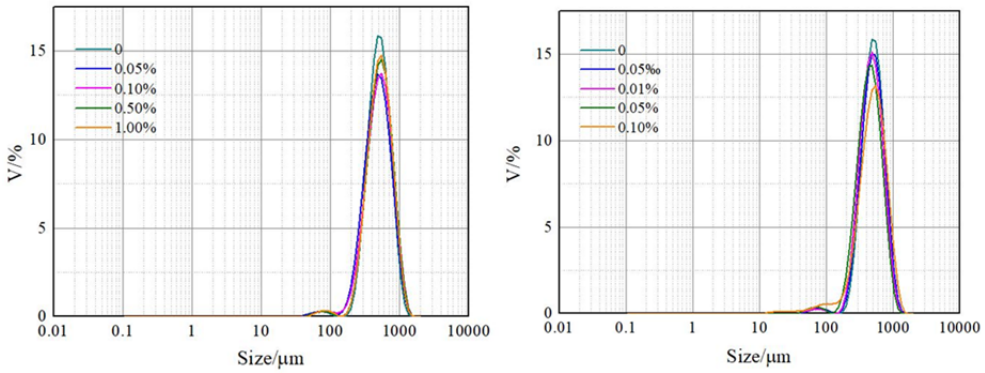

a *b*

Figure 5: Particle size distribution graphs of Na_2SO_4 products at 130 ˚C and 300 rpm with different impurity ions: a, K^+; b, F^-

In addition to the three main inorganic salts, there are some other inorganic ions in the wastewater, K^+ and F^- being the main impurity ions. Based on the concentration of these two ions in wastewater, the evaporation crystallization of Na_2SO_4 were conducted with different amount of impurity ions. Figure 5 displays the corresponding particle size distribution of Na_2SO_4 products.

Table 4: Particle size distribution of Na_2SO_4 products at 130 ˚C and 300 rpm with different impurity ions

Impurity	Condition	$D_{0.10}$/μm	$D_{0.16}$ /μm	$D_{0.50}$ /μm	$D_{0.84}$ /μm	D(4,3)/μm	C.V./%
wt.%(K^+)	0	309	343	502	724	529	37.95
	0.05	268	307	483	734	516	44.20
	0.10	280	323	512	775	544	44.14
	0.50	302	341	522	775	554	41.57
	1.00	301	340	517	761	547	40.72
wt.%(F^-)	0	309	343	502	724	529	37.95
	0.005	293	330	495	726	524	40.00
	0.01	281	315	471	693	499	40.13
	0.05	253	287	442	658	469	41.97
	0.10	249	300	499	765	526	46.59

As shown in Table 4, the addition of impurity ions can cause a decrease in $D_{0.10}$, whether it is K^+ or F^-. Specifically, $D_{0.10}$ increases with the increasing wt.%(K^+). But when wt.%(K^+) reaches 0.500%, continuing to increase the concentration of K^+ has no significant effect on $D_{0.10}$. The different effect between these two ions is that $D_{0.10}$ gradually decreases as wt.%(F^-) increases.

3.4 Effect of organics on evaporation crystallization process

In addition to a large amount of inorganic salts, high-saline wastewater also contains complex organic pollutants. Based on the analytical report, tributyl phosphate, 4-methyl-2-pentanone, dodecane and p-nitrophenol were selected as targeted organics. The evaporation crystallization process was carried out at 130 °C and 300 rpm, and 10 mM different organic substances were added respectively. Figure 6 and Table 5 show that the addition of organic matter leads to a decrease in $D_{0.10}$. Furthermore, the degree of influence is ranked as tributyl phosphate> 4-methyl-2-pentanone> dodecane> p-nitrophenol.

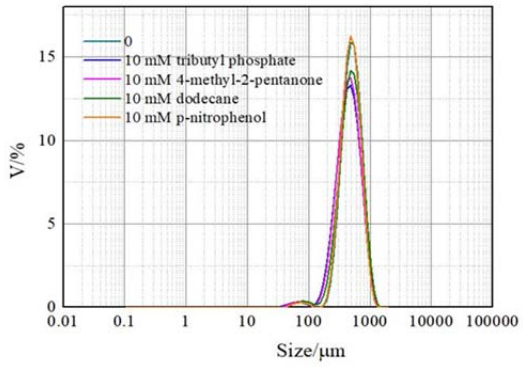

Figure 6: Particle size distribution graph of Na_2SO_4 products at 130 ˚C and 300 rpm with organics

Table 5: Particle size distribution of Na_2SO_4 products at 130 ˚C and 300 rpm with organics

Condition	$D_{0.10}$/μm	$D_{0.16}$ /μm	$D_{0.50}$ /μm	$D_{0.84}$ /μm	D(4,3)/μm	C.V./%
No additives	309	343	502	724	529	37.95
10 mM Tributyl phosphate	243	279	447	686	478	45.53
10 mM 4-methyl-2-pentanone	248	284	447	677	476	43.96
10 mM dodecane	273	312	485	725	513	42.58
10 mM p-nitrophenol	298	332	485	693	509	37.22

In addition, the crystal morphology was characterized by SEM. Figure 7 indicates that organic matter of 10 mM has no significant effect on the morphology of Na_2SO_4 products. In the actual production process, the evaporation mother liquor will be recycled. With the progress of evaporation, the organic matter will be

continuously enriched. Therefore, the effect of high concentration organic matter on Na_2SO_4 should be investigated in future.

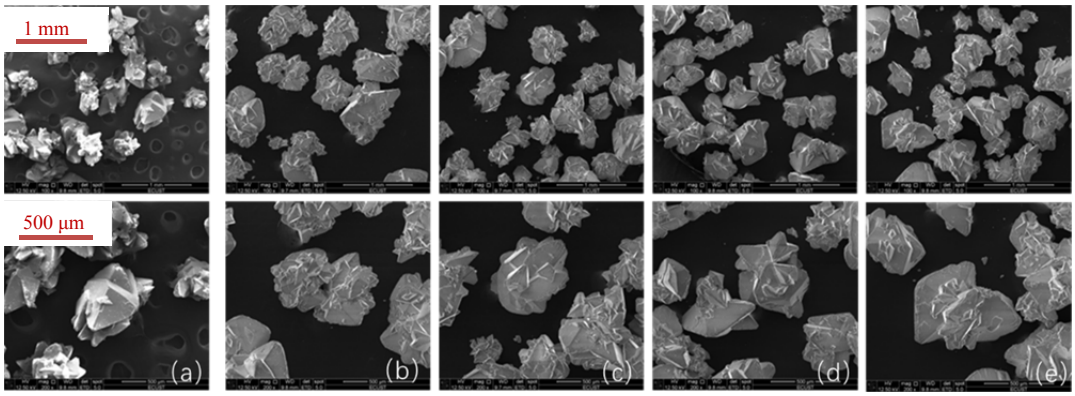

Figure 7: SEM graphs of Na_2SO_4 products: a, No additives; b, 10 mM Tributyl phosphate; c, 10 mM 4-methyl-2-pentanone; d, 10 mM dodecane; e, 10 mM p-nitrophenol

4. Conclusions

The recycling of Na_2SO_4 in high-saline system NaCl-$NaNO_3$-Na_2SO_4-H_2O can be achieved by evaporation crystallization process, and the purity of unwashed product is over 99.0%. The relationships between evaporation and time at 118, 120 and 130 °C were measured respectively, indicating the evaporation efficiencies at different heating temperatures. In the temperature range of 115-150 °C, $D_{0.10}$ of Na_2SO_4 increases with increasing temperature, reaches maximum at 130 ˚C, and then it gradually decreases. Considering the evaporation efficiency and the particle size distribution of Na_2SO_4 products, the optimum heating temperature was determined to be 130 ˚C. Similarly, 300 rpm was chosen as the optimum stirring rate, because $D_{0.10}$ increases first and then decreases with increasing stirring rate. In addition, the effects of impurity ions and organic matter on the preparation of Na_2SO_4 were also discussed. On the whole, the addition of impurity, whether ions or organic matter, can lead to a decrease of $D_{0.10}$. In particular, $D_{0.10}$ increases with the increasing wt.%(K^+) in the range of 0.05%-1.00%, while $D_{0.10}$ gradually decreases as wt.%(F^-) increases in the range of 0.005%-0.10%. The degree of influence of organic matter on $D_{0.10}$ is ranked as Tributyl phosphate> 4-methyl-2-pentanone> dodecane> p-nitrophenol. However, the addition of 10 mM organic matter has little effect on the morphology of Na_2SO_4 products. Further study is required because the organic matter will be continuously enriched in the actual production process.

Acknowledgments

The authors acknowledge the financial supports sponsored by Shanghai Academic/ Technology Research Leader (Grant No. 18XD1424600), Shanghai Sailing Program (Grant No. 17YF1403200), and the Fundamental Research Funds for the Central Universities (Grant No. WB1717008).

References

Bian C., Chen H., Song X. F., Jin Y., Yu J. G., 2018, Stable phase equilibria of the quaternary system Na+//Cl–, NO3–, SO42—H2O at 353.15 K, Journal of Chemical & Engineering Data, 63, 3305-3314.

Lin W. Y., Bo W. M., Li H., Huang X. L., 2011, Study on the metastable phase equilibria of the quaternary system Na+//NO3–, Cl–, SO42—H2O at 25 and 50 °C, Gaoxiao Huaxue Gongcheng Xuebao, 25, 376-379.

Song P. S., Huang X. L., 2007, Thermodynamic model and prediction of solubilities in the system of Na+, K+, Mg2+//NO3–, Cl–, SO42-–H2O at 298.16 K II. Pitzer mixing parameters for the system Na+, K+//NO3–, Cl––H2O and their applications, Yanhu Yanjiu, 15, 29-33.

Yang J., Wang Y. F., Shu M., Yang L. B., Zhu L., Zhao X. Y., Sha Z. L., 2017, Solid-liquid equilibrium of Na+//Cl–, NO3–, SO42-–H2O quaternary system at 373.15 K, Fluid Phase Equilibria, 445, 7-13.

Zhang X., Huang X. L., 2015, Study on the phase equilibria of the quaternary system Na+//Cl–, SO42-, NO3—H2O at low temperatures, Huaxue Tongbao, 78, 337-341.